Small systems, small sensors

Oomen, Pieter Edmond

Chapter 3

Generic, resealable microfluidic system for perfusion culture of cells and tissues

Maciej D. Skolimowski, Pieter E. Oomen, Hylke Waalewijn, Viktoriia Starokozhko, Marjolijn T. Merema, Martin Dufva, Arto Heiskanen, Jenny Emnéus, Geny M. M. Groothuis, Elisabeth Verpoorte

To be submitted

Abstract

The development of *in vitro* systems for the incubation of tissue and cell cultures is of great interest to the pharmaceutical industry. In an effort to decrease the attrition rate of drug candidates, they can be used to assess pharmacodynamics, metabolism and toxicology of compounds at an early stage during development. Microfluidics can be applied to develop highly *in vivo*-like environments, incorporating flow and allowing researchers to exert great control over their incubation experiments. However, many systems lack user-friendliness, and most are only suitable for tissue or cell culture, but not both. We present a generic, resealable microfluidic system that allows facile incubation of tissue slices and hydrogel-embedded cell cultures under flow. The system was used in conjunction with poly(dimethylsiloxane) and polycarbonate biochips, which were used for the incubation of precision-cut liver slices and 3D HepG2 cultures, respectively. A clamp allowed swift opening and closing of the culture chambers for the insertion of cells or tissue. Compared to traditional well-plate incubation in static medium, both precision-cut liver slices and 3D HepG2 cultures remained viable over at least 24 hours and 42 hours, respectively. The system includes a peristaltic pump, medium reservoirs and sample containers, and the possibility to equilibrate medium used for perfusion with a gas mixture of choice.

PEO designed the study and system with MDS, performed some of the experiments and coordinated writing / finalization of the manuscript.

3.1 Introduction

There is a growing demand in several medical research fields to mimic *in vivo* functionality more accurately *in vitro*. One such example is regenerative medicine, in which the medical focus lies on restoring the impaired function of cells, tissue or organs *in vivo* .[1] The possibility of cultivating *in vivo*-quality organ tissue *in vitro* from a patient's own stem cells, enabled by microfluidic technology, would be a great solution for the many patients waiting for suitable donor organs. This approach would have the additional advantage that the potential risk of graft rejection would be substantially diminished.[2] There is also interest in pharmaceutical industry to develop better predictive models for preclinical drug testing. *Ex-vivo* models that better mimic the interaction of human organs with drugs would aid in the more efficient selection of novel therapeutic agents that are safe for patients. Furthermore, it would finally become possible to interrogate the intricate *in vivo* biological signalling system in healthy versus diseased patient tissue using sophisticated analytical techniques designed for *in vitro* applications. The drive to develop *in vitro* systems that best resemble the *in vivo* situation has thus sparked innovation not only in the field of tissue engineering, but also in the fabrication of tools, development of new biomaterials and the reduction of animal testing.[3] The largest potential application for the development of human *in vitro* models, especially those representing the liver, continues to be in the pharmaceutical industry.[4] Only 10% of the compounds reaching the clinical testing phase involving human subjects actually make it to the market, due mostly to the poor predictive power of common preclinical test approaches.[5–9] The costs of clinical testing far exceed those of preclinical testing. As a consequence, the further the drug advances in testing stages, the more expensive a possible failure becomes. Therefore, methods that better predict not only the pharmacodynamics, but also the absorption, distribution, metabolism, excretion and toxicology (ADME-Tox) of a new drug at an early stage in its development are of great interest.[9,10] The attrition rate could thus be decreased through the development of better *in vitro* liver models.

The combination of microfluidics, fabrication techniques and tissue engineering has led to a new generation of advanced *in vitro* test systems known as organs-on-chips, devices which reproduce organ function *in vitro*.[6] Instead of taking the conventional approach of 2D cell cultures submerged in medium on well plates, organ-on-a-chip systems often employ perfusion and use one or more cell types to cultivate tissue on 3D scaffolds. The resulting systems better recreate the *in vivo* niche, and can be used as platforms to identify and validate the efficacy and safety of potential drug compounds early on, for eventual progression to clinical trials.[11] There are two general approaches to creating these systems, namely a "top-down" approach using organ tissue in perfusable systems, and the "bottom-up" approach employing (3D) cell cultures to mimic tissue functions.[12–14]

The "top-down" biological approach to organ-on-a-chip systems is used in our labs for pharmacokinetic and toxicological studies. Precision-cut liver slices (PCLS) of human or mammalian origin, representing the whole organ,[15] are conventionally submerged in medium in well plates, one slice per well, and incubated at 37 °C and in an atmosphere of 80 to 95% O_2 and 5% CO_2. Viability can be sustained for several days, provided an optimum medium composition is used,[16,17] and most metabolic pathways remain stable for at least 24 h.[15] A major advantage of PCLS is that tissue architecture is well preserved, with all the different cell types and extracellular matrix in the original tissue present, as well as the activity of endogenous enzymes particularly important for drug metabolism. Van Midwoud *et al.* realized a systematic improvement to the well-plate format by developing a continuous-flow microfluidic system for perifusion

of PCLS.[18] (We refer to slice "perifusion" rather than "perfusion" as the medium flows around the slice, which is freely suspended in the culture chamber, rather than through it.) An advantage of this system in comparison to conventional well-plate incubation is that medium composition is constant, but can be easily changed during incubation to include potential drug compounds and/or enzyme inhibitors and inducers. Continuous addition of nutrients and removal of waste products and metabolites are also easily achieved. Additional advantages of this system include the possibility to do in-line analysis of metabolites[19] and to implement studies investigating organ interactions.[20] Other "top-down" organ-on-a-chip work has been aimed at the study of ethanol toxicity on liver explants[21], as well as chemotherapy evaluation on incubated cancer biopsies.[22] A more advanced system was recently reported by Astolfi *et al.*[23], in which micro-dissected tumor tissue was incubated in well-traps. In this case, no flow was used for tissue incubation, and the system was employed to assess chemotherapeutics in an effort to achieve personalized therapy.

"Bottom-up" biological approaches are more common. 2D and, increasingly, 3D cell (co)cultures are being employed to recreate tissue functionality and predict pharmacodynamics and ADME-Tox. Generally, some form of scaffold or hydrogel is used to encourage the growth of cell cultures in 3D.[13,24] In one example, a complex microfluidic device was developed to expose several liver carcinoma (HepG2) cell cultures in parallel microchambers to gradients of anti-cancer compounds in order to increase the throughput of drug screening experiments.[25] However, not all cell types (*e.g.* HepG2) are suitable for predictive ADME-Tox studies, due to the decreased expression of the relevant metabolic enzymes and lack of a retained 3D structure, in contrast to PCLS.[18,26] It has been shown that, as with tissue explants, exposure to flow is beneficial for maintaining the functional activity of HepG2 cell cultures.[27,28] Culture of cell types representing different tissue types in separate compartments in "bottom-up" devices has also been reported. The relatively simple, compartmentalized, microfluidic culture of liver (HepG2) and intestinal (Caco-2) cell lines was used to study transport processes of xenobiotics to achieve more *in vivo*-like multi-organ metabolism of certain compounds.[29] More advanced devices can even comprise interconnected long-term co-culture of cells representing four different tissue types[30] or be used to assess the safety of repeated drug exposure[31]. Liver organoids consisting of cultured HepG2 and NIH-3T3 fibroblasts have also been cultured in hydrogels on a digital microfluidic platform, which allowed precise actuation of the organoids and mixing with drugs.[32] With these co-cultures, careful control over the medium and extracellular matrix compounds and provision of the necessary mechanical cues using microfabrication can lead to highly *in vivo*-like systems.

One recurring issue in this kind of microfluidic *in vitro* system is complexity, and an associated lack of user-friendliness. To date, the biological model has dictated microfluidic system design, and the development of generic systems has taken a back seat. This has led to the presentation of a number of systems in the literature that are well developed for a very specific perfusion culture, only to rapidly disappear again once the particular study in question has been published. An exception to this was a more generic modular design for microfluidics applications developed by Sabourin *et al.*; however, this system has not yet been widely adopted.[33] Moreover, to the best of our knowledge, there is no microfluidic system that allows for both cell and tissue culture for different applications. In this work, our aim was to develop a user-friendly, integrated, perfusion microsystem concept which can be used for both "top-down" and "bottom-up" biological approaches. The flow-through microchamber device for cell and tissue incubation consists of an upper and lower half, which can be easily assembled and resealed

by mounting in a commercially available clamp. We demonstrate the application of our microfluidic perfusion system concept for two very different experiments, namely studies using PCLS, and cultivation of 3D HepG2 cell cultures embedded in hydrogel. In the former case, a poly(dimethylsiloxane) (PDMS) device was cast by injection into a micromilled polycarbonate (PC) mold. In the latter case, a very similar device, but then micromilled in PC, was used for 3D liver cell culture.

3.2 Materials and methods

All chemical reagents, unless stated otherwise, were obtained from Sigma-Aldrich, The Netherlands.

3.2.1 System design

To demonstrate our generic, resealable incubation system, two different embodiments were developed. One was a gas-permeable PDMS biochip for the incubation of PCLS, whereas the other was a gas-impermeable PC biochip for 3D HepG2 cell cultures. PDMS was chosen for PCLS in order to assure the passive supply of the high oxygen concentrations necessary for slice incubation by diffusion through this material.[34,35] PC was chosen for HepG2 in order to demonstrate the realization of our generic device in other biocompatible materials (and thus by other fabrication means) as well. Elements similar to the PCLS biochip developed by van Midwoud *et al.* were incorporated in both biochips.[18] Each system features six individually addressable culture chambers with integrated, porous PC membranes. One of these membranes is incorporated near the bottom of the chamber just after the inlet, while the other is located near the top of the chamber, just before the outlet. Together, the membranes enable an even flow distribution of medium through these chambers (Fig. 1). Both the PDMS and PC biochips were manufactured in two halves, which can be assembled by clamping in a Fluidic Connect PRO77 holder (Micronit Microfluidics BV, Enschede, Netherlands) to allow leakage-free perfusion of the culture chambers. This clamping system also allows swift opening and closing of the devices for the easy and efficient introduction of cells and tissue samples (*vide infra*, Fig. 4C).

The microfluidic system comprises five functional exchangeable blocks, including the multichamber biochip, medium reservoirs (one block each for the inlet and outlet), a container to serve as an incubator for generation of controlled gaseous atmospheres, and peristaltic pumps; these blocks are connected by a maximum of sixteen fluidic lines (Fig. 2). The culture medium is transported from the reservoirs using up to two 8-channel, peristaltic micropumps actuated by miniature DC motors (LEGO A/S, Denmark) described previously[36,37] to the multichamber biochips. The holder with the biochip can be placed inside a small, sealed, plastic box that allows equilibration of medium with a gas mixture of choice, by purging the interior using tubing inserted into holes made in the box. The system can thus be used outside gas-controlled incubators, and only needs to be kept at 37° C. In the case of the PDMS device, medium equilibration with 95% oxygen and 5% carbon dioxide for PCLS experiments occurs by diffusion of these gases over the biochip walls directly into the medium in the chamber. For experiments in PC chambers medium oxygenation was done by diffusion over the walls of silicone tubing (1 m long, 400 μm thick walls, ID 500 μm, Da Vinci, The Netherlands) used to deliver medium to the biochips. The parts of the assembled system not containing microfeatures (holders for the reservoirs and pump) were 3D-printed (Felix 3.0, FELIXrobotics, The Netherlands) in polylactic acid (PLA, EasyFill filaments, Formfutura V.O.F., The Netherlands). All structures in PC (*i.e.* HepG2 biochip, parts of the pump and moulds for casting of PDMS) were fabricated using micromilling (Mini-Mill/3PRO, Minitech Machinery Corp.,

USA) from EPRAFORM PC (Eriks, The Netherlands). All micro-milled features had a 100 µm tolerance.

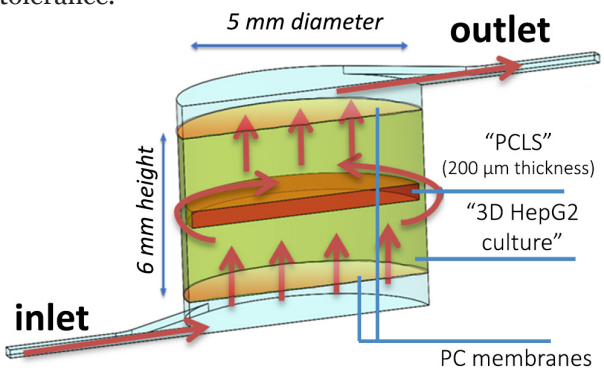

Figure 1: Concept of slice perifusion and cell perfusion as implemented in the PDMS and PC biochips. In both cases, an inlet from below supplies a culture microchamber with fresh medium, with an outlet at the top. The diameter of the culture chamber is 5 mm and the height 6 mm, giving rise to volumes of about 120 µL. The volume between the upper and lower PC membranes (10 µm thick, 8-µm pores) occupied by the slice or cells is 75 µL. Indicated are the approximate size and position of a PCLS in the culture chamber (orange) as well as a 3D HepG2 culture in gel (green). The red lines indicate flow of medium through the culture chamber, through embedded 3D HepG2 cultures, but around incubated PCLS (perifusion).

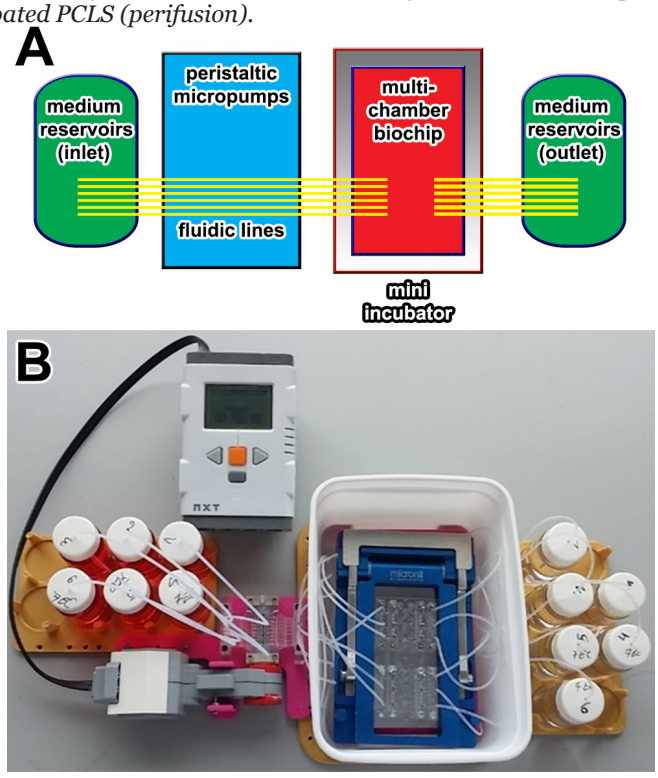

Figure 2: (A) Microfluidic system design, here showing 6 fluidic lines. (B) The assembled microfluidic system with 6-chamber PC biochip and single peristaltic pump. The box containing the clamp can be purged (when sealed with a lid) with a gas mixture of choice, after which equilibration of medium occurs over the walls of the device (PDMS biochip) or through silicone tubing (PC biochip).

3.2.1.1 PDMS biochip

The PDMS biochips for incubation of tissue slices were fabricated by casting in micromilled, PC moulds. The PDMS (Sylgard 184, Dow Corning Corp., USA) was prepared by mixing prepolymer with curing agent in a 10:1 weight ratio and degassing under vacuum for 20 minutes, before injection into the moulds and curing at 70°C for 2h. Fig. 3 illustrates the fabrication process of the two complementary halves used to make the biochips for the incubation of PCLS. Each half had the same design. To ensure even distribution of medium as it is introduced to the culture chamber (or exits from it again), a droplet-shaped inlet (or outlet) chamber was created in the lower half of the mould, with the pointed end facing the inlet opening. A PC membrane was inserted over this inlet. (In the complementary half of the device, the PC membrane is located just before the outlet of the piece.) These membranes (8-µm pores, 10 µm thick) were cut from larger membranes (Millipore, Amsterdam, The Netherlands). To make a PDMS part, a membrane was aligned between the structures for chamber formation in the two mould parts. The two parts of the hollow mould were then brought together and tightly sealed using screws, squeezing the PC membrane securely between them. In this way, blocking of the PC membrane with uncured PDMS was prevented when PDMS prepolymer solution was injected into the mould (Fig. 3B and C). The volume between the membranes was approximately 75 µL. The exterior surfaces of the two chamber halves were sealed off by bonding a 1-mm-thick slab of PDMS (Fig. 3F) to them. An oxygen-plasma treatment (Harrick Plasma, Ithaca, NY) of the surfaces to be bonded ensured a permanent seal between the slab and the moulded chamber, as has been described in the literature .[38] This resulted in one PDMS biochip containing three culture chambers, with dimensions 30 x 25 x 6 mm. In order to fit two sets of the PDMS biochips (compare Fig. 2B) in the clamp, aluminum parts were milled (see Fig. 3G). This resulted in a system with six individually addressable culture chambers. The fabrication process is significantly easier than the original design by van Midwoud *et al.*, which involved the manual alignment and bonding of 10 layers to achieve the two parts making up the slice chambers.

3.2.1.2 PC biochip

Figure 4 shows the design of the PC biochip. Figure 4A shows an exploded view of the individual milled parts and how they align with each other to form the two halves of a PC biochip. Figure 4B is a cross-sectional view of one of the chambers. After milling of the PC parts, the upper and lower halves were bonded using a method described by Ogończyk *et al.*[39] In brief, the polycarbonate surfaces were exposed to chloroform vapour in a closed vessel at room temperature for 5 min. As with the PDMS biochip, PC membranes were put in place in the six culture chambers, again resulting in a volume between the membranes of approximately 75 µL. Next, the substrates were left for 30 minutes outside the container in a fumehood to allow excess solvent to evaporate. The bonding was performed by using a hot-embossing press (Dr. Collin GmbH, Germany). The parts were sandwiched between two steel plates, placed in the press and heated up to 140°C. After that, 3.2 MPa pressure was applied for 20 min. After the press was allowed to cool down to room temperature, the pressure was released. The two halves of the device were assembled by mounting them in the upper and lower jaws of the clamp. Leakage of medium between the two halves of the PC biochip was prevented by the insertion of small PDMS gaskets at the interface between the two parts. The PC fluidic connectors were also milled, and PDMS was cast into the hollow interior of these connectors from underneath (see Fig. 4B). This allowed leakage-free connection of tubing to supply medium to the culture chambers. The

channels conducting medium to the culture chambers were 1 mm wide and 1.2 mm high. The connectors were attached to the PC biochip using screws.

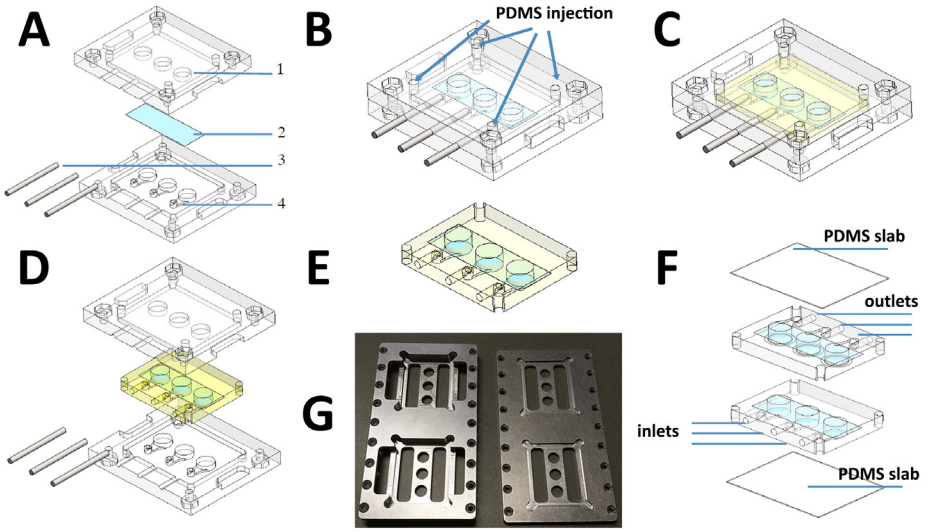

Figure 3: Fabrication of the microfluidic PDMS biochip for the perifusion of PCLS. (A) The milled, PC mould parts (1,4) sandwich a PC membrane (2). 1.5-mm-diameter stainless steel rods (3) are inserted from the side before casting to create inlets for tubing. (B) The two parts are screwed together and uncured, degassed PDMS is injected through the holes indicated with arrows. (C) The PDMS (yellow) is cured at 70° C for 2 h. (D) The mold is unscrewed and the rods are removed to yield the PDMS biochip component. (E) One half of the PDMS biochip for PCLS incubation with integrated PC membrane. The second half containing the other half of the chamber is prepared in the same manner. Note that the chamber is still completely open. (F) A 1-mm-thick slab of PDMS closes each half of the biochip, sealing one side of the chamber to form the bottom or top of the assembled biochip. Tubing can be inserted into the inlets to allow perfusion of the culture chambers with medium. (G) This photo shows the milled, aluminum inserts for the clamping system, between which two sets of 3-chamber PDMS biochips can be fixed. The aluminum inserts are fixed in the upper and lower jaws of the Fluid Connect Pro clamp, which can be swiftly opened and closed using the handle (see Fig. 4C for a photograph of the open clamp).

3.2.2 Tissue cultures

3.2.2.1 Preparation of precision-cut liver slices (PCLS)

All experiments were approved by the Animal Ethical Committee of the University of Groningen. PCLS preparation was performed based on the protocol by De Graaf *et al.*[40] In brief, male Wistar rats (300 g, free access to food and water) (Charles River, Netherlands) were anaesthetized using isofluorane/O_2 and the liver was excised. The liver was stored in ice-cold University of Wisconsin (UW) solution (DuPont Critical Care, USA). Cylindrical cores were removed from the liver using a hollow drill bit. These 5-mm-diameter cores were transferred to a Krumdieck slicer (Alabama R&D, USA). The collection reservoir of the slicer was filled with ice-cold Krebs-Henseleit buffer[41] with D-glucose (25 mM, Merck, Germany), $NaHCO_3$ (25 mM, Merck) and HEPES (10 mM, MP Biomedicals, USA) added. This buffer was saturated with 95% O_2 and 5% CO_2. The cores were sliced into PCLS with a thickness of approximately 200 µm (about 10 cell layers) and a wet weight of 5 mg. PCLS were stored for a maximum of 24 hours in ice-cold UW

solution until further experiments. We have previously shown that this procedure preserves the viability and metabolic functionality of liver slices.[40]

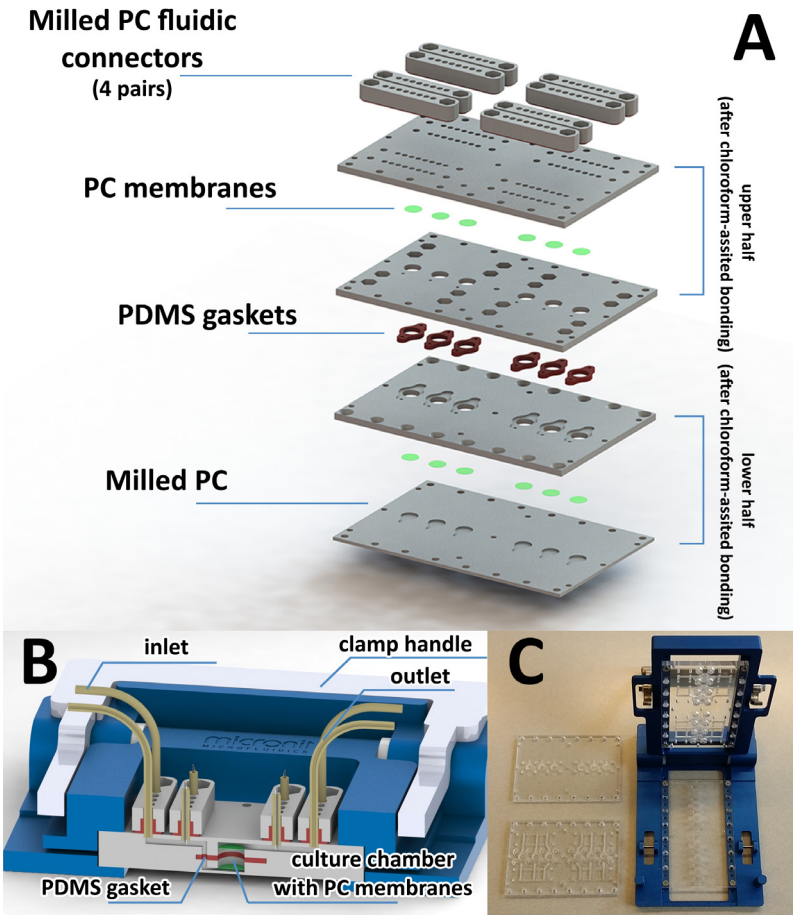

Figure 4: The PC biochip for incubation of 3D HepG2 cultures. (A) An exploded view showing the individual parts of the biochip. Four extra milled PC fluidic connectors are designed for future applications, but are not used in this work. (B) A cross-section of one of the six culture chambers in the biochip, showing the fluidic architecture. (C) A photograph of the PC biochip in the Fluidic Connect Pro. This clamp consists of two jaws joined at the back by a hinge. One half of the device is mounted in the upper jaw of this clamp, whereas the other half is mounted in the lower jaw. By bringing the handle of the clamp backwards, the jaws, and thus the two device halves, are brought together and closed. A PDMS gasket positioned around each chamber in the lower half of the device ensures leakage-free operation once the clamp is completely closed, due to the elastomeric property of this silicone material.

3.2.2.2 PCLS incubation in the PDMS biochip

All incubations were performed at 37 °C. Slices were individually pre-incubated in 12-wells plates for a period of 1 hour. Each well with slice contained 1.3 mL of Williams' medium E (WME, GlutaMAX™ Supplement, Gibco, ThermoFisher Scientific, The Netherlands), which was saturated (carbogenated) with humidified 80% O_2 and 5% CO_2 gas. This pre-incubation removes cellular debris resulting from the slicing procedure and also recovers the intracellular levels of

ATP to pre-excision levels.[42] To ensure efficient oxygenation of the medium, the entire incubator (Panasonic, Japan) containing the well plates was shaken at 90 rpm, and the atmosphere kept at 80% O_2/5% CO_2. The biochip was perfused with medium for one hour at 37 °C in an incubator built in-house to thermally equilibrate the system before slices were placed in the separate chambers of the biochip. Medium was pumped using the LEGO-driven peristaltic micropump. The complete clamping system with biochip was placed in a polypropylene box which was then sealed with a lid. The clamp was placed on top of tissues wet with water to maintain a high level of humidity inside the box to prevent evaporation of medium. The closed box containing the gas-permeable PDMS biochip was purged during experiments with humidified carbogen gas (95% O_2 and 5% CO_2) to oxygenate medium by diffusion of oxygen through the walls of the silicone tubing (used to conduct medium to the biochip) and the biochip itself. After slice pre-incubation, medium flow was temporarily stopped to the biochip chambers, and the device was opened by opening the clamp. A slice was transferred into each chamber from the well plate used for pre-incubation. The biochips were then immediately sealed by closing the clamp, and medium flow was started again. PCLS were also transferred to individual wells of a new 12-well plate with 1.3 mL of fresh, warm, oxygen- and carbon dioxide-equilibrated WME medium in each well. During experiments, slices were perifused for 24 hours with a flowrate of 600 µL/h. Control slices were incubated in well plates for 24 hours. For each experiment as well as for the control, a set of 3 slices per set of conditions was used and the experiment was repeated 3 times with 3 individual livers (n=3*3).

3.2.3 HepG2 cell cultures in the PC chip

3.2.3.1 Preparation of HepG2 cell cultures

HepG2 cells (liver carcinoma cells, passage 35-40; ATCC HB-8065, Thermo Fischer SCIENTIFIC, USA) were transferred from the original line of cells to a culture flask (25 cm^2, Corning® cell culture flasks) and incubated in 5 mL of RPMI medium with 1% penicillin/streptomycin and 10% fetal bovine serum (FBS, Sigma-Aldrich, USA) added, in a controlled incubation environment (37°C, humidified air supplemented with 5% CO_2). The cells were cultured in this controlled environment until the cells covered the bottom surface of the flask (approximately 3-4 days). The growth medium was removed, and PBS with 0.05% trypsin (Sigma-Aldrich, USA) was added to detach the cells. The cells were suspended in 5 mL RPMI-FBS medium, transferred to a 15-mL Falcon tube and centrifuged for 5 min at 1100 rpm. The supernatant was then removed, and the cell pellet was resuspended in 1 mL of medium. From this concentrated cell suspension, new culture flasks were seeded.

3.2.3.2 HepG2 hydrogel embedment and incubation

HepG2 cells were incubated in 0.5% and 2% calcium alginate hydrogels. HepG2 cells were embedded in these gels by first growing cells in culture flasks as described above, and preparing a 4 million cells/mL suspension in cell culture medium. Meanwhile, alginate (Alginic acid sodium salt, Sigma-Aldrich) was dissolved in water to 1% and 4% w/w solutions, and autoclaved. The cell suspension and alginate solutions were mixed in a 1:1 ratio to create a suspension containing 2 million cells in 2% alginate and a suspension containing 2 million cells in 0.5% alginate. The suspensions were seeded to either a well in a 48-well plate (50 µL) or a culture chamber in the PC biochip (30 µL); these different volumes were used in order to compensate for the size disparity between the culture chambers in the

biochip and the wells, and create comparable gel thicknesses. The alginate in the solution was gelled by adding equal amounts of 50 mM calcium chloride solution to the cell suspensions, embedding the cells in the gel. Using this concentration of calcium chloride, gelling was instant and the incubation was started immediately after gelling. As in the case of PCLS incubation, the biochip mounted in the clamping system was perfused using a peristaltic pumping system. Again, HepG2 cultures were also incubated in well plates as control. In the biochip, a flow rate of 600 µL/hr was used. Both the perfused and static cultures were incubated at 37° C, in air with 5% CO_2. No separate box for the biochip was necessary, as the whole flow setup was placed in the incubator.

3.2.4 Viability studies

3.2.4.1 ATP content

The adenosine triphosphate (ATP) content of slices is an indicator of viability, since ATP is the primary transporter of chemical energy in cells.[44] ATP analysis of PCLS was performed using the ATP Bioluminescence Assay Kit (CLS II, Roche), containing luciferase and ATP standard solution. After performing PCLS experiments, slices were harvested and stored in a safelock vial (Eppendorf, Germany) containing 1 mL solution containing 2 mM EDTA in a 70% ethanol/H_2O solution at pH 10.9 and 1-mm-diameter glass beads. The vial was immediately frozen in liquid nitrogen. The slices were stored at -80°C until further analysis was performed. Before ATP analysis, the samples were thawed on ice. Luciferase was thawed at room temperature. The samples were homogenized using a mini-bead beater for 40 sec (Biospec Products, USA) and centrifuged (Eppendorf, Germany) for 5 min at 4°C and 13,200 rpm. Five-µL aliquots of each sample (supernatant) and of a positive control (a standard slice sample) were then pipetted into separate wells (in duplicate). Forty-five (45) µL of 0.1 M Tris (Merck) HCl buffer with 2 mM EDTA (pH 7.8) were added to each of the sample wells. A calibration curve was prepared according to the manufacturer instructions, using dilutions of the ATP standard solution from the kit in 0.1 M Tris HCl buffer with 2 mM EDTA (pH 7.8). Fifty µL of each ATP standard was added in duplicate to separate wells in black 96-well plates (Costar, Fisher Scientific, USA). Fifty µL of luciferase were added to all the wells to start the reaction. The luminescence was measured after 5 minutes using a luminometer (Lumicount microplate luminometer, Packard, USA) and the concentrations of ATP calculated. The results of the ATP analysis were normalized using the protein content of each sample slice to correct for differences in size between slices. Differences between different flow conditions were tested for statistical significance ($p \leq 0.05$) using a Student's t-test.

3.2.4.2 Protein analysis

Protein analysis was performed based on Lowry's method[45], using the BIO-rad DC Protein Assay kit (BIO-rad, Germany). After the ATP measurement (*vide supra*) was completed, the supernatant was removed and the pellet was dried overnight at 37°C. The dried precipitate was treated with 200 µL of 5M NaOH and incubated for 30 min in a 37° C water bath. The samples were diluted to 1 mL with ultrapure water (18.2 MΩ·cm at 25° C), and the sample was homogenized again using a mini-bead beater for 40 seconds. Standards for measurement of a calibration curve were prepared from a stock solution of bovine serum albumin (ICN Biomedicals Inc., USA). Five-µL aliquots of slice samples and bovine serum albumin standards were pipetted into a clear 96-well plate (Costar) in duplicate. After this, reagent A and B were added according to the instructions of the manufacturer. Absorbance was measured at 650 nm in a ThermoMax Microplate

Reader (Molecular Devices, USA), after which the protein content of each slice was calculated.

3.2.4.3 HepG2 live-dead staining

Live-dead staining was performed to assess cell viability and culture growth at two time points during the incubation experiments; 22 and 42 hours. For these experiments, a LIVE/DEAD Cell Imaging Kit (Life Technologies, The Netherlands) was used. After incubating cells with the dyes for 15 minutes at room temperature, images were taken using a fluorescence microscope (AxioObserverZ1, Carl Zeiss, Germany) with an EC plan-Neonfluar 5x/0.16 Ph 1 objective. The excitation wavelengths for the imaging of live and dead cells were 470 nm and 538-562 nm, respectively. The emission wavelengths were 500-527 nm and 570-640 nm, respectively. Cell counting was performed after processing the images with the freeware, ImageJ, and the ICTN plugin (http://rsb.info.nih.gov/ij/plugins/itcn.html). Each channel (green for living cells and red for dead cells) was converted to 8-bit color depth, inverted and changed to grey-scale. Differences between the results obtained under different conditions were tested for statistical significance ($p \leq 0.05$) using a Student's t-test. A more in-depth protocol of the image analysis is provided in the Supplementary Information at the end of this chapter.

3.3 Results and discussion

Two sets of cultivation experiments were performed to demonstrate proof-of-concept for this microfluidic perfusion device. One set was performed in a PDMS embodiment, and involved incubation of rat PCLS. The other set of experiments was performed in PC embodiment of the device with human hepatocyte cancer (HepG2) cell cultures.

3.3.1 PCLS viability in the PDMS device

PCLS were cultured under flow in the second-generation biochips made of PDMS, and under static conditions using polystyrene 12-well plates. Their viability was determined by the analysis of cellular ATP content after 24 h of incubation in either the biochip or a 12-well plate. The bar chart in Figure 5 shows the results of this assay.

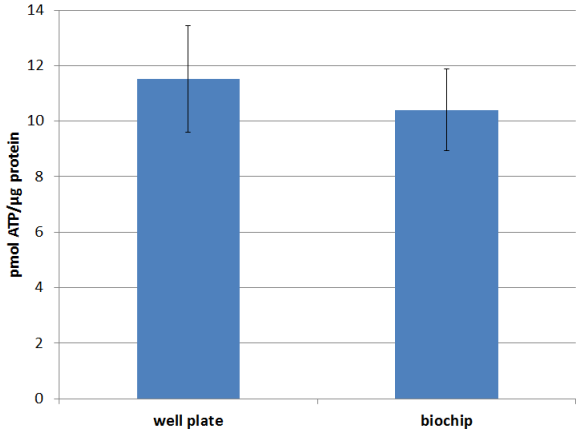

Figure 5: Bar chart of PCLS incubation experiments in 12-well-plate and microfluidic biochip formats. Slices were perifused with medium in the biochip for 24 h at 600 µL/h. The ATP content of incubated slices was normalized for slice protein content (pmol ATP/µg protein). ATP levels in the slices perifused in the biochip are comparable to those found for PCLS controls in 12-well plates. The bars show averages (n=3) ± SEM.

The results show that the ATP/protein content of slices incubated in the biochip is similar to those incubated in well plates. Furthermore, the absolute amount of ATP per slice falls in the range of 10-12 pmol/µg protein, values which agree with those generally obtained in our lab .[40] We can conclude that the slice had sufficient access to oxygen and was preserved during the 24 h incubation period.[46] Interestingly, pmol ATP/ µg protein levels of slices incubated in the original PDMS biochips by van Midwoud *et al.*[18] were found to be lower than those in well plates in previous, unpublished studies in our labs. In contrast, incubating PCLS in the new, resealable PDMS biochip with clamping system yields similar pmol ATP/µg protein levels for slices in wells and biochips. This is possibly a result of the markedly improved procedure for insertion of slices using the clamping system. Using the earlier system, opening the biochip, inserting slices and closing the biochip again could take up to 15 minutes, during which time slices were exposed to ambient conditions. In the PDMS devices presented here, this takes no more than 5 minutes. The results from the ATP assay appear to be confirmed by preliminary measurements of lactate dehydrogenase (LDH) leakage into the medium (another viability assay). This will be further investigated in future experiments.

3.3.2 HepG2 3D cell culture viability in the PC device

HepG2 cells were cultured under flow in the PC device and under static conditions in well plates, embedded in alginate hydrogels as described above. After staining, fluorescence microscopy images were taken 1 hour after embedding the cells in the hydrogel and after 70 hours of incubation in both the biochip and well plate (see Fig. 6). Live cells are shown as green and dead cells as red. The increased size of the cultures after 70 hours suggests cell proliferation, confirming viability and growth of the embedded cell cultures in both biochip and well plate in both hydrogel compositions. This effect is more pronounced in the biochip, in which cells had been perfused at 600 µL/hr. We observed a less homogeneous distribution of cells in the 0.5% gel compared to the 2.0% gel in the biochip after 70 hours, with large 3D cell clusters observed in the former, less

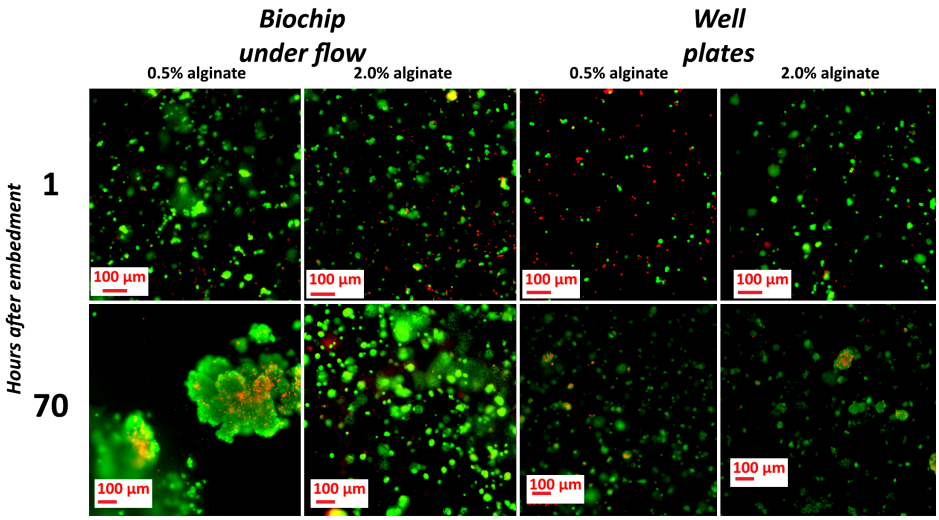

Figure 6: Fluorescent images of HepG2 cells embedded in 0.5% and 2.0% alginate gels, 1 hour and 70 hours after incubation. The colors represent viable (green) and dead (red) cells. Formation and growth of cell clusters and agglomerates can be observed, indicating viability and proliferation of the cells.

stiff matrix. It was observed that the formation of large clusters leads to lower survival of cells in the central regions of these clusters. This is likely caused by insufficient supply of nutrients and oxygen to these regions due to slow diffusion. However, the majority of cells remain viable over a period of 70 hours as tested in this experiment. Fewer dead cells were observed after 70 hours in the 2.0% gel in the biochip, possibly because no large clusters were formed (Fig. 6), ensuring adequate oxygen and nutrient supply.[32]

In order to quantify the observed cell growth, the average area of cell cultures in fluorescent microscope images was compared for different flow regimes and hydrogel concentrations as described above (Fig. 7).

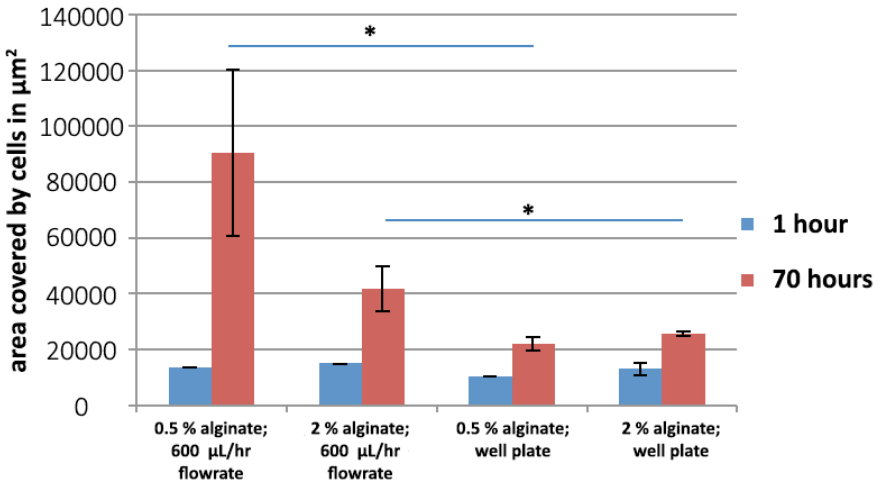

Figure 7: Area covered by HepG2 cells in µm2 after 1 and 70 hours, showing the growth of cultures during incubation (n=3 for each set of conditions). Cultures grown under flow (600 µL/hr) exhibit significantly increased cell growth compared to the well plate setup (no flow) (marked with ""). No significant difference in the culture growth between the 0.5% alginate and 2.0% alginate hydrogels was found, independent of culture conditions. All bars show averages (n=3) ± SD.*

The results confirm that cells cultured under flow exhibit significantly more proliferation than cells in the static well plate setup. This is likely due to the flow of medium, which facilitates direct and continuous delivery of enough oxygen and nutrients to keep cells proliferating, while simultaneously removing metabolic waste from the incubation environment. Our observation that perfusion at moderate flow rates enhances cell culture is in line with other authors.[27,28,51] In general, this can also be considered to be more comparable to the *in vivo* situation in liver tissue.

As the 2.0% alginate hydrogel-embedment appeared to give the most desirable results, the ratio of live and dead cells was ascertained after 22 and 42 hours of incubation in this matrix. For this, stained cultures were imaged using fluorescence microscopy (Fig. 8). The results of the quantitative analysis of live:dead cell ratios are given in Fig. 9.

Cell cultures incubated under flow exhibit significantly better viability than those incubated under stagnant conditions. This confirms the earlier reported superior viability exhibited by cultures incubated under flow.[27,28,51]

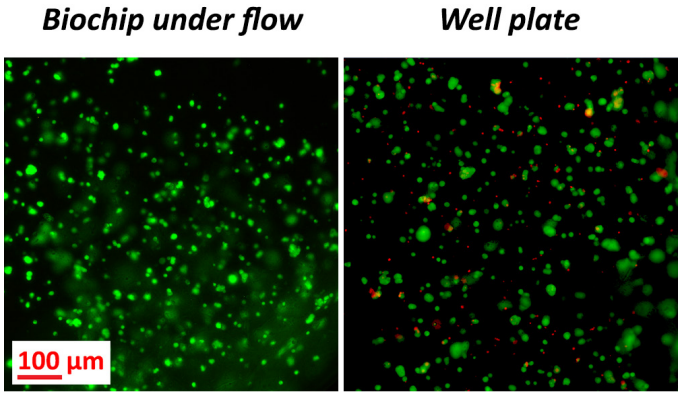

Figure 8: Representative fluorescence micrographs of HepG2 cells in 2% alginate hydrogels after 42 hours of incubation under flow in the PC biochip or in well plates.

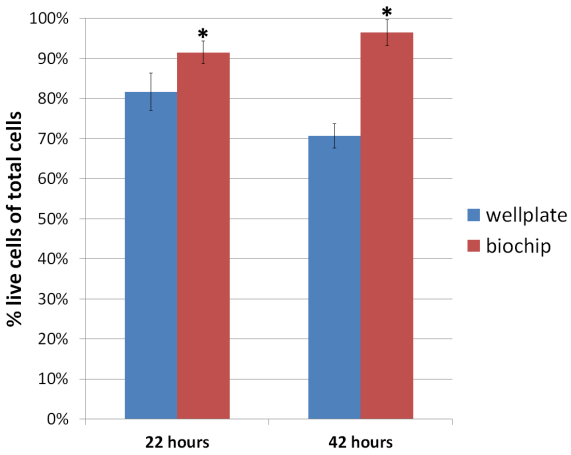

Figure 9: Comparison of live cells in 2.0% alginate culture, in biochip and well plate, after 22 and 42 hours of incubation (averages (n=3) ± SD). Bars marked with "" indicate significant differences between the well plate and biochip incubation systems.*

3.4 Conclusions

As was alluded to in the introduction, one of the main barriers in popularizing microfluidic devices for mass-scale *in vitro* drug screening might be the lack of a generic system that bridges the gaps between models of different biological complexity. The presented generic, resealable microfluidic system for perfusion culture of cells and tissues was shown to allow flexible and effective incubation of different cell and tissue models in biochips of different materials. Unique for this system is that it enables perfusion culture of both *in vitro* liver cell and tissue models, allowing comparison between different levels of biological complexity. This creates opportunities for future research with organ-on-a-chip systems, as different biological materials can be tested using the same basic setup. Combined with the great ease of use created through the employment of a universal chip clamp, this approach will contribute to the further application of microfluidics to *in vitro* research.

The improved design of the PDMS biochip proved to be very suitable for culturing tissue slices. PCLS ATP/protein levels data exhibit improved viability in the new system compared to previous versions of the biochip. ATP levels are

similar to PCLS incubated in well plates, which is considered the benchmark setup for viability comparisons.[18] The growth of gel-embedded HepG2 cell cultures in the system with a PC biochip was compared to the growth of cells in a well plate setup. It was found that the perfused biochip system is significantly better in supporting growth in alginate hydrogel compared to the well plate setup. The viability of HepG2 cells in the biochip was compared with that in the well plate using live/dead staining. As was hypothesized, the continuous flow environment of the system improved cell viability in the 3D cell culture. The live:dead cell ratio of cultures embedded in 2.0% alginate hydrogel and exposed to flow was higher than in similarly embedded cultures incubated under static conditions in well plates.

The results from this study provide a good basis to continue experiments with this setup. It demonstrates the possibility to create viable 3D cell cultures, with the essential capability to recreate optimal nutrient delivery for generation of artificial tissue.[52,53] Confirming the functionality of these cell cultures will be the next experimental step. Future experiments should also show if different cell types, like primary human hepatocytes, can be cultured in the system. The slicing procedure used for the preparation of PCLS has been used on various other tissue types.[20,54–56] Exploring compartmentalized cultures of different tissue types and their interactions in a biochip with interconnected chambers is of great interest, and could form a piece of the puzzle to mimic the response of the entire human body to a drug.

3.5 Acknowledgements

We thank Micronit B.V. for the use of their micromilling machine.

3.6 References

1 A. S. Daar and H. L. Greenwood, *J. Tissue Eng. Regen. Med.*, 2007, **1**, 179–184.
2 C. N. Svendsen, *Hum. Mol. Genet.*, 2013, **22**, 32–38.
3 L. G. Griffith, A. Wells and D. B. Stolz, *Hepatology*, 2014, **3**, 1426–1434.
4 K. Domansky, W. Inman, J. Serdy, A. Dash, M. H. M. Lim and L. G. Griffith, *Lab Chip*, 2010, **10**, 51–8.
5 P. Y. Muller and M. N. Milton, *Nat. Rev. Drug Discov.*, 2012, **11**, 751–761.
6 E. W. Esch, A. Bahinski and D. Huh, *Nat. Rev. Drug Discov.*, 2015, **14**, 248–260.
7 J. Bowes, A. J. Brown, J. Hamon, W. Jarolimek, A. Sridhar, G. Waldron and S. Whitebread, *Nat. Rev. Drug Discov.*, 2012, **11**, 909–22.
8 G. Caponigro and W. R. Sellers, *Nat. Rev. Drug Discov.*, 2011, **10**, 179–187.
9 I. Kola and J. Landis, *Nat. Rev. Drug Discov.*, 2004, **3**, 711–715.
10 P. M. van Midwoud, E. Verpoorte and G. M. M. Groothuis, *Integr. Biol. (Camb).*, 2011, **3**, 509–21.
11 A. D. van der Meer and A. van den Berg, *Integr. Biol.*, 2012, **4**, 461-470.
12 E. Verpoorte, P. E. Oomen, M. D. Skolimowski, P. P. M. F. A. Mulder, P. M. van Midwoud, V. Starokozhko, M. T. Merema, G. Molema and G. M. M. Groothuis, in *Transducers 2015: 18th International Conference on Solid-State Sensors, Actuators and Microsystems*, Anchorage, Alaska, USA, 2015, pp. 224–227.
13 N. Alépée, A. Bahinski, M. Daneshian, B. de Wever, E. Fritsche, A. Goldberg, J. Hansmann, T. Hartung, J. Haycock, H. T. Hogberg, L. Hoelting, J. M. Kelm, S. Kadereit, E. McVey, R. Landsiedel, M. Leist, M. Lübberstedt, F. Noor, C. Pellevoisin, D. Petersohn, U. Pfannenbecker, K. Reisinger, T. Ramirez, B. Rothen-Rutishauser, M. Schäfer-Korting, K. Zeilinger and M.-G. Zurich, *ALTEX*, 2014, **31**, 441–77.
14 U. Marx, T. B. Andersson, A. Bahinski, M. Beilmann, F. R. Cassee, M. Cirit, M. Daneshian, O. Frey, C. Gaertner, C. Giese, L. Griffith, T. Hartung, M. B. Heringa, J. Hoeng, W. H. de Jong, J. Kuehnl, M. Leist, A. Luch, I. Maschmeyer and A. Roth, *ALTEX*, 2016, **33**, 1–64.

15 I. A. M. de Graaf, G. M. M. Groothuis and P. Olinga, *Expert Opin. Drug Metab. Toxicol.*, 2007, **3**, 879–898.
16 V. Starokozhko, G. B. Abza, H. C. Maessen, M. T. Merema, F. Kuper and G. M. M. Groothuis, *Toxicol. In Vitro*, 2015, **30**, 288–299.
17 V. Starokozhko, S. Vatakuti, B. H. Schievink, M. T. Merema, A. Asplund, J. Synnergren, A. Aspegren and G. M. M. Groothuis, *Arch. Toxicol.*, 2016. DOI 10.1007/s00204-016-1865-x.
18 P. M. van Midwoud, G. M. M. Groothuis, M. T. Merema and E. Verpoorte, *Biotechnol. Bioeng.*, 2010, **105**, 184–94.
19 P. M. van Midwoud, J. Janssen, M. T. Merema, I. A. M. de Graaf, G. M. M. Groothuis and E. Verpoorte, *Anal. Chem.*, 2010, **83**, 84–91.
20 P. M. van Midwoud, M. T. Merema, E. Verpoorte and G. M. M. Groothuis, *Lab Chip*, 2010, **10**, 2778–86.
21 S. M. Hattersley, J. Greenman and S. J. Haswell, *Biomed. Microdevices*, 2011, **13**, 1005–14.
22 S. M. Hattersley, D. C. Sylvester, C. E. Dyer, N. D. Stafford, S. J. Haswell and J. Greenman, *Ann. Biomed. Eng.*, 2012, **40**, 1277–1288.
23 M. Astolfi, B. Péant, M. A. Lateef, N. Rousset, J. Kendall-Dupont, E. Carmona, F. Monet, F. Saad, D. Provencher, A.-M. Mes-Masson and T. Gervais, *Lab Chip*, 2015, **16**, 312–325.
24 F. Pampaloni, E. G. Reynaud and E. H. K. Stelzer, *Nat. Rev. Mol. Cell Biol.*, 2007, **8**, 839–45.
25 N. Ye, J. Qin, W. Shi, X. Liu and B. Lin, *Lab Chip*, 2007, **7**, 1696–1704.
26 H. H. J. Gerets, K. Tilmant, B. Gerin, H. Chanteux, B. O. Depelchin, S. Dhalluin and F. A. Atienzar, *Cell Biol. Toxicol.*, 2012, **28**, 69–87.
27 J. M. Prot, C. Aninat, L. Griscom, F. Razan, C. Brochot, C. G. Guillouzo, C. Legallais, A. Corlu and E. Leclerc, *Biotechnol. Bioeng.*, 2011, **108**, 1704–15.
28 R. Jellali, T. Bricks, S. Jacques, M.-J. Fleury, P. Paullier, F. Merlier and E. Leclerc, *Biopharm. Drug Dispos.*, 2016, **37**, 264–275.
29 T. Bricks, P. Paullier, A. Legendre, M. J. Fleury, P. Zeller, F. Merlier, P. M. Anton and E. Leclerc, *Toxicol. in Vitro*, 2014, **28**, 885–895.
30 I. Maschmeyer, A. K. Lorenz, K. Schimek, T. Hasenberg, A. P. Ramme, J. Hübner, M. Lindner, C. Drewell, S. Bauer, A. Thomas, N. S. Sambo, F. Sonntag, R. Lauster and U. Marx, *Lab Chip*, 2015, **15**, 2688–2699.
31 I. Maschmeyer, T. Hasenberg, A. Jaenicke, M. Lindner, A. K. Lorenz, J. Zech, L. A. Garbe, F. Sonntag, P. Hayden, S. Ayehunie, R. Lauster, U. Marx and E. M. Materne, *Eur. J. Pharm. Biopharm.*, 2015, **95**, 77–87.
32 S. H. Au, M. D. Chamberlain, S. Mahesh, M. V. Sefton and A. R. Wheeler, *Lab Chip*, 2014, **14**, 3290–9.
33 D. Sabourin, P. Skafte-Pedersen, M. J. Søe, M. Hemmingsen, M. Alberti, V. Coman, J. Petersen, J. Emnéus, J. P. Kutter, D. Snakenborg, F. Jørgensen, C. Clausen, K. Holmstrøm and M. Dufva, *J. Lab. Autom.*, 2013, **18**, 212–228.
34 E. Szalowska, G. Stoopen, J. C. W. Rijk, S. Wang, P. J. M. Hendriksen, M. J. Groot, J. Ossenkoppele and A. A. C. M. Peijnenburg, *Toxicol. Vitr.*, 2013, **27**, 1513–24.
35 H. Martin and J. Sarsat, *Cell Biol. Toxicol.*, 2002, **18**, 73–85.
36 P. Skafte-Pedersen, D. Sabourin, M. Dufva and D. Snakenborg, *Lab Chip*, 2009, **9**, 3003–3006.
37 M. Skolimowski, M. Weiss Nielsen, F. Abeille, P. Skafte-Pedersen, D. Sabourin, A. Fercher, D. Papkovsky, S. Molin, R. Taboryski, C. Sternberg, M. Dufva, O. Geschke and J. Emnéus, *Biomicrofluidics*, 2012, **6**, 34109.
38 D. C. Duffy, J. C. McDonald, O. J. A. Schueller and G. M. Whitesides, *Anal. Chem.*, 1998, **70**, 4974–4984.
39 D. Ogończyk, J. Wegrzyn, P. Jankowski, B. Dabrowski and P. Garstecki, *Lab Chip*, 2010, **10**, 1324–1327.
40 I. A. M. de Graaf, P. Olinga, M. H. de Jager, M. T. Merema, R. de Kanter, E. G. van de Kerkhof and G. M. M. Groothuis, *Nat. Protoc.*, 2010, **5**, 1540–51.
41 L. E. Bailey and S. D. Ong, *J. Pharmacol. Methods*, 1978, **1**, 171–175.

42 D. K. Obatomi, S. Brant, V. Anthonypillai, D. A. Early and P. H. Bach, *Toxicol. in Vitro*, 1998, **12**, 725–737.
43 P. M. van Midwoud, M. T. Merema, N. Verweij, G. M. M. Groothuis and E. Verpoorte, *Biotechnol. Bioeng.*, 2011, **108**, 1404–12.
44 B. Alberts, A. Johnson, J. Lewis, M. Raff, K. Roberts and P. Walter, *Molecular Biology of the Cell*, Garland Science, New York, NY, 4th edn., 2002.
45 O. H. Lowry, N. J. Rosebrough, A. L. Farr and R. J. Randall, *J. Biol. Chem.*, 1951, **193**, 265–275.
46 D. F. Wilson, D. K. Harrison and S. A. Vinogradov, *J. Appl. Physiol.*, 2012, **113**, 1838–45.
47 F. K.-M. Chan, K. Moriwaki and M. J. De Rosa, 2013, **979**, 65–70.
48 S. R. Caliari and J. A. Burdick, *Nat. Methods*, 2016, **13**, 405–14.
49 F. Molina-Jimenez, I. Benedicto, V. L. Dao Thi, V. Gondar, D. Lavillette, J. J. Marin, O. Briz, R. Moreno-Otero, R. Aldabe, T. F. Baumert, F. L. Cosset, M. Lopez-Cabrera and P. L. Majano, *Virology*, 2012, **425**, 31–39.
50 A. Kinasiewicz, J. Kawiak and A. Werynski, *Biocybern. Biomed. Eng.*, 2006, **26**, 47-55.
51 M. S. Kim, J. H. Yeon and J. K. Park, *Biomed. Microdevices*, 2007, **9**, 25–34.
52 T. Hongo, M. Kajikawa, S. Ishida, S. Ozawa, Y. Ohno, J.-I. Sawada, A. Umezawa, Y. Ishikawa, T. Kobayashi and H. Honda, *J. Biosci. Bioeng.*, 2005, **99**, 237–244.
53 L. G. Griffith and M. A. Swartz, *Nat. Rev. Mol. Cell Biol.*, 2006, **7**, 211–224.
54 R. de Kanter, M. Monshouwer, A. L. Draaisma, M. H. de Jager, I. A. M. de Graaf, J. H. Proost, D. K. F. Meijer and G. M. M. Groothuis, *Xenobiotica.*, 2004, **34**, 229–241.
55 A. R. Parrish, A. J. Gandolfi and K. Brendel, *Life Sci.*, 1995, **57**, 1887–1901.
56 N. Parajuli and W. Doppler, *Vitr. Cell. Dev. Biol. - Anim.*, 2009, **45**, 442–450.

Chapter 3 - Supplementary Information

S3.1 Detailed description of image analysis

Images were processed using the software Zeiss ZEN (black edition, Carl Zeiss, Germany) and exported to ImageJ software to perform cell counting and assessment of cell proliferation. Cell counting was performed after image processing using the freeware ImageJ and the ICTN plugin (http://rsb.info.nih.gov/ij/plugins/itcn.html). Each channel (green for living cells and red for dead cells) was converted to 8-bit color depth, inverted and changed to a grey scale. The cells were counted using ICTN plugin. Figure 1 shows the different image processing steps required for cell counting.

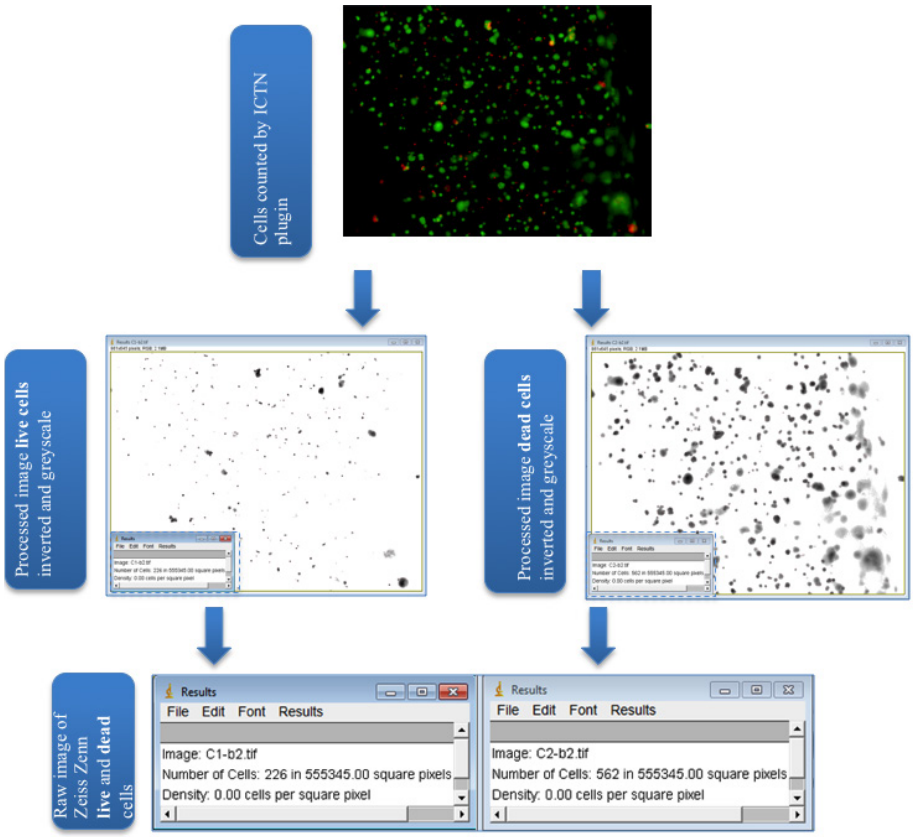

Figure S1: Cell counting using ICTN plugin for ImageJ

Cell proliferation was assessed by determining the growth of cell clusters (or clumps of cells) in the images using a protocol created by the Otago Centre for Confocal Microscopy.[1] In brief, a threshold was selected to remove background noise from the live channel images. To correct for parts of the picture where no cells were present, a region of interest (ROI) was selected with constant size for every picture (400x400 pixels, approximately 600x600 µm). For every analyzed picture, the positioning of the ROI was chosen to yield an area as large as possible. If multiple areas in a picture could be selected this was done to increase the power of the test. Assuming all cells are roughly the same size, this gives information

about the number of cells within the ROI. Figure 2 shows an example of how the conversion was performed.

1. A. McNaughton, “Measuring Area Using Thresholds,” http://occm.otago.ac.nz/resources/ImageJ-Thresholding.pdf (accessed March 2016)

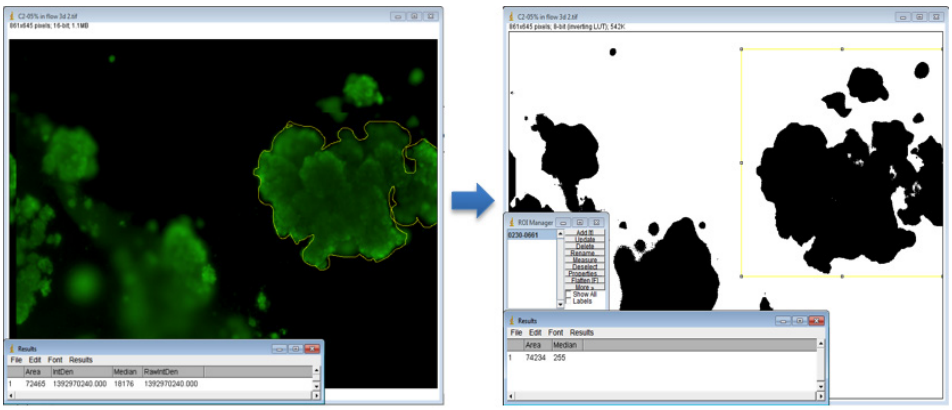

Figure S2. Conversion of the ‘live channel’ using a threshold value. The left image also shows an area measured by manually outlining the culture. The resulting areas are comparable, but using the threshold value to assess culture area is much faster.